

Stability of Bubble Nuclei through Shell-Effects *

Klaus Dietrich and Krzysztof Pomorski †
 Technische Universität München, Garching, Germany

Abstract

We investigate the shell structure of bubble nuclei in simple phenomenological shell models and study their binding energy as a function of the radii and of the number of neutron and protons using Strutinsky's method. Shell effects come about, on the one hand, by the high degeneracy of levels with large angular momentum and, on the other, by the big energy gaps between states with a different number of radial nodes. Shell energies down to -40 MeV are shown to occur for certain magic nuclei. Estimates demonstrate that the calculated shell effects for certain magic numbers of constituents are probably large enough to produce stability against fission, α -, and β -decay. No bubble solutions are found for mass number $A \leq 450$.

PACS numbers: 21.10.Sf, 24.10.Nz, 47.20.Dr, 47.55.DZ

1 Introduction

The possibility that nuclei could exist in the form of a (spherical) bubble or in the form of a toroid has been pointed out long ago [1,2]. Within the liquid drop model (LDM) nuclei of these shapes turn out to be unstable with respect to deformations. Shell-effects may, however, stabilize such nuclei against deformation.

In a series of papers [3], C.Y. Wong investigated shell-effects for toroidal and bubble-shaped nuclei using Strutinsky's shell correction method. He restricted his attention to known nuclei near the valley of β -stability and found that for certain doubly magic nuclei (${}^{200}_{80}\text{Hg}_{120}$, ${}^{138}_{58}\text{Ce}_{80}$) spherical bubble solutions with a very small inner radius (ratio of inner to outer radius ≈ 0.07) turned out to be the ground state. Indications that bubble solutions might exist were also found in mean field calculations [4] and for stellar matter at finite temperature [5]. More recently, Moretto et al. [6] showed in a classical model that LD-bubbles at finite temperature may be stabilized by an internal vapor pressure.

In the present paper, we study shell effects for nuclear bubbles in a broad range of neutron (N) and proton (Z) numbers extending considerably beyond the known nuclei. As C.Y. Wong we make use of Strutinsky's shell correction method [7]. We show that the

*We dedicate this paper to Prof. Richard Lemmer on the occasion of his 65th birthday.

†On leave on absence from University M.C.S. in Lublin

shell energy may become as large as -40 MeV for certain magic numbers of the nuclear constituents and that nuclear bubbles may thus become stable or very long-lived against fission and other decay modes.

2 Theory

In Strutinsky's method [7], the total binding energy E of a nucleus (neutron number N , proton number Z , nucleon number A) of given shape is given as a sum of the liquid drop (LD) energy $E_{\text{LD}}(N, Z)$ and the shell correction energy δE_{shell}

$$E(N, Z) = E_{\text{LD}}(N, Z) + \delta E_{\text{shell}}(N, Z) . \quad (1)$$

The shell correction energy has the well-known form [7]

$$\delta E_{\text{shell}} = \sum_{\nu} e_{\nu} \delta n_{\nu} , \quad (2)$$

where e_{ν} are the single particle energies and δn_{ν} is the difference between the occupation numbers $n_{\nu} = \theta_0(e_F - e_{\nu})$ in the shell-model ground state and a smooth distribution \bar{n}_{ν}

$$\delta n_{\nu} = n_{\nu} - \bar{n}_{\nu} . \quad (3)$$

The smooth occupation pattern is defined in the usual way as a functional of a smooth level distribution [7].

We use the Strutinsky method to study the total energy and especially the shell correction energy of spherical nuclear bubbles. The single particle energies e_{ν} as well as the LD energy depend on the inner (R_2) and outer (R_1) radius of the bubble nucleus. Adopting the conventional saturation condition that the volume of the LD remains constant independently of its shape, the two radii are related by the condition

$$R_1^3 - R_2^3 = R_0^3 , \quad (4)$$

where $R_0 = r_0 A^{1/3}$ is the radius of a compact spherical nucleus of the same mass. We describe the shape of the bubble nucleus either by the dimensionless radii

$$v_{1(2)} := \frac{R_{1(2)}}{R_0} \quad (5)$$

or by the ratio f between the volume of the hole and the volume of the entire bubble

$$f := \frac{R_2^3}{R_1^3} . \quad (6)$$

The difference ΔE_{LD} between the energy of the LD-bubble and the energy of the corresponding compact spherical LD is given by

$$\Delta E_{\text{LD}} = E_S(R_1, R_2) + E_{\text{Cb}}(R_1, R_2) - E_S(R_0) - E_{\text{Cb}}(R_0) , \quad (7)$$

where E_S and E_{Cb} are the surface and Coulomb energies of the bubble and the compact configuration, resp. Measuring ΔE_{LD} in units of the surface energy $E_S(R_0)$ and substituting the explicit form of the different energies, we find

$$\mathcal{E} := \frac{\Delta E_{LD}}{E_S(R_0)} = v_1^2(v_2) + v_2^2 - 1 + 2X_0 \left[v_1^5(v_2) + \frac{3}{2}v_2^5 - \frac{5}{2}v_2^3v_1^2(v_2) - 1 \right], \quad (8)$$

where

$$v_1(v_2) := [1 + v_2^3]^{\frac{1}{3}} \quad (9)$$

and X_0 is the conventional fissility parameter

$$X_0 \equiv \frac{E_{Cb}(R_0)}{2E_S(R_0)} = \frac{Z^2/A}{(Z^2/A)_{\text{crit}}} \quad (10)$$

with

$$(Z^2/A)_{\text{crit}} := \frac{40\pi\sigma r_0^3}{3e_0^2}. \quad (11)$$

The quantities σ , r_0 , and e_0 are the surface constant, the radius parameter, and the elementary charge, resp.. Beside the trivial solution $v_2 = 0$ (compact spherical nucleus) the condition of stationarity

$$\frac{\partial \mathcal{E}}{\partial v_2} = 0 \quad (12)$$

has real solutions $v_2(X_0)$ only for $X_0 > 2.02$. They represent a multivalued function which is shown in the l.h.s. of Fig. 1 for a limited range of values $v_2(X_0)$. For given $X_0 > 2.02$ the smallest solution $v_2(X_0) \leq 0.4$ corresponds to the maximum of the potential barrier, whereas the next solution in magnitude $v_2(X_0) > 0.4$ corresponds to a minimum of the energy \mathcal{E} for a bubble of the reduced radius $v_2(X_0)$.

On the r.h.s. of Fig. 1 we show the energy change \mathcal{E} by bubble formation as a function of v_2 . For $X_0 > 2.2$, the bubble solution is seen to correspond to a lower energy than the one of a compact sphere ($v_2 = 0$). The barrier between the bubble solution and the compact spherical one occurs for reduced inner radii in the interval $0 \leq v_2 \leq 0.4$. In units of $E_S(R_0)$ the barrier heights are seen to be at most at $\mathcal{E} = 0.025$. The unit $E_S = 4\pi\sigma R_0^2$ is, however, pretty large. For $A = 580$, $Z = 280$ and reasonable values of the parameters r_0 and σ , we have $E_S = 1291$ MeV and $X_0 = 2.62$. The corresponding energies of the barrier and the minimum are ~ 20 MeV and ~ -140 MeV. It is not meaningful to pursue the solutions v_2 of Eq. (12) to values of v_2 and X_0 much larger than the ones given in Fig. 1, because for increasing X_0 the charge density of the bubble turns out to be unphysically large and the diameter $d = R_1 - R_2$ of the bubble layer becomes unphysically small.

We emphasize that the bubble solutions obtained in the LDM are not stable with respect to deformations [3] in the same way as the compact spherical liquid drops are not stable against fission for fissibility parameters $X_0 > 1$. Nevertheless, stability can in principle be produced by shell effects.

As two extreme and simple cases of nuclear single particle potentials we consider the shell effects in an infinite square well and in a harmonic oscillator:

$$V(r) = \begin{cases} -V_0 & \text{for } R_2 < r < R_1 \\ +\infty & \text{otherwise} \end{cases} \quad (13)$$

$$V(r) = -V_0 + \frac{M\omega^2}{2}(r - \bar{R})^2. \quad (14)$$

The depth $V_0 > 0$ has no influence on the shell correction energy and can thus be put equal to zero. The center of the oscillator potential is chosen to be

$$\bar{R} = \frac{R_1 + R_2}{2}. \quad (15)$$

The oscillator frequency ω is chosen in such a way that the RMS deviation from the sphere of radius \bar{R} is the same when calculated with the shell model wave function and with the LD-density

$$\langle (r - \bar{R})^2 \rangle_{\text{SM}} = \langle (r - \bar{R}) \rangle_{\text{LD}}. \quad (16)$$

We have to add a spin-orbit term to the central potential (13) or (14). We use the conventional form in the Skyrme approach (see Eq. (5.103) in Ref. [8])

$$\hat{V}_{\text{SO}} = \tilde{V}_{\text{SO}}(r) \hat{l} \cdot \hat{s}, \quad (17)$$

$$\tilde{V}_{\text{SO}}(r) = \frac{3}{2} W_0 \frac{1}{r} \frac{\partial \rho(r)}{\partial r}, \quad (18)$$

$\rho(r)$ is the nuclear density distribution. We choose the value $W_0 = 120 \text{ MeV fm}^5$ given in Ref. [8] and neglect the isospin dependence which is recently under debate [9].

For the total density $\rho(r)$ which appears in the expression for the spin-orbit potential $\tilde{V}_{\text{SO}}(r)$ (Eq. (18)) we used the following ansatz:

$$\rho(r) = \rho_0 \left[1 - 2 \left(\frac{r - \bar{R}}{R_1 - R_2} \right)^2 \right] \quad (19)$$

where $\rho_0 = 0.17 \text{ fm}^{-3}$ and \bar{R} is given by Eq. (15). For simplicity we have assumed that the proton and neutron densities ρ_p and ρ_n are proportional to Z or N respectively.

It is seen from (18) that the sign of the spin-orbit potential is opposite in the inner and outer surface region of the bubble nucleus. Consequently, the magnitude of the spin-orbit splitting is smaller for bubble nuclei than for normal ones. We, therefore, treat the spin-orbit term in perturbation theory. The eigenenergies e_{nlj} of the s.p. Hamiltonian including the spin-orbit potential (17) and the unperturbed eigenvalues ε_{nl} are related by the equation

$$e_{nlj} = \varepsilon_{nl} + \langle \psi_{nljm} | \tilde{V}_{\text{SO}} | \psi_{nljm} \rangle \cdot \left(j(j+1) - l(l+1) - \frac{3}{4} \right), \quad (20)$$

where $(n - 1)$ represents the number of radial nodes (not counting zeros at $r = 0, \infty$) and l, j, m are the orbital and total angular momentum and its projection, resp.. The mean value $\langle \psi_{nljm} | \tilde{V}_{\text{SO}} | \psi_{nljm} \rangle$ depends only on the unperturbed s.p. density

$$\rho_{nl}(r) = \psi_{nljm}^+(\vec{r}) \psi_{nljm}(\vec{r}) = \frac{u_{nl}^2(r)}{r^2} . \quad (21)$$

The functions $u_{nl}(r)$ satisfy the radial Schrödinger equation with eigenvalue ε_{nl} . For the infinite square well the eigenvalues and eigenfunctions are obtained by numerically satisfying the boundary conditions and for the harmonic oscillator (14) we used the WKB approximation.

3 Results and Discussion

We complement the results obtained in the pure LDM (see Fig. 1) by Fig. 2 which shows lines of equal LD-binding energy per particle ($E_{\text{LD}}(N, Z)/A$) as a function of N and Z . We note that the volume term of the LDM is present in this figure since we do not subtract the energy of the compact spherical LD. The LD parameters are taken from Ref. [10]. Each point on the equipotential lines corresponds to a spherical bubble solution as given by the LDM, which is unstable with respect to deformations. It should be noted that the largest energy gains per particle occur for nucleon numbers $1200 \leq A \leq 2000$ and the corresponding proton numbers $325 \leq Z \leq 400$. Some of the isobaric lines are cut twice by the same equi-energy line. If the binding energy per particle in between these 2 points is smaller, a β -stable isobar lies somewhere on this section. Of course, this consideration is thwarted by the fact, that the LD-bubbles are all unstable against fission. In the LDM, the (spherical) bubble solutions are saddle points, not minima.

The LD results (and consequently also the result on the total binding energy) depend sensitively on the value of the surface constant σ . This surface constant contains a poorly known isospin-dependent part. In our calculations we adopted the isospin dependence given by Myers and Swiatecki [10] who write the surface energy of a spherical LD in the form

$$E_S(R_0) = 17.9439 \text{ MeV} \cdot A^{2/3} \left[1 - 1.7826 \left(\frac{N - Z}{A} \right)^2 \right] \quad (22)$$

In Fig. 3 we show the spectrum of single particle levels for the shifted infinite square well with a spin-orbit term. The levels are shown as a function of the hole fraction parameter f (see Eq. (6)). As f increases, the diameter $d = R_2 - R_1$ of the bubble layer decreases. Increasing the number of radial nodes for given orbital angular momentum l thus costs an energy which rises steeply as a function of f . Augmenting a given l -value by 1 for given n and given parameter f implies an increase of the centrifugal energy, which is the larger, the larger the l -value. Magic numbers come about by the interplay between levels e_{nlj} with $n \geq 2$, which rise rapidly as a function of f and levels e_{1lj} , which depend more gently on f with a tendency to decrease with f due to the diminishing centrifugal energy.

In Fig. 4, we display a corresponding level spectrum for the harmonic oscillator potential. The general trends are the same as for the infinite square well, but the magic numbers for the same values f differ for the square well and oscillator. This is not surprising. A Saxon-Woods form centered around \bar{R} would be more realistic and the magic numbers for this choice would be expected to lie between the limits given by the infinite square well and the oscillator.

For both the potentials we observe that the spin-orbit splitting is often reversed as compared to the case of normal nuclei. The reason was already given in Section 2. The shell correction energy δE_{shell} is shown as a function of N (or Z) at a given value of $f = 0.28$ for the infinite square well in Fig. 5 and for the harmonic oscillator in Fig. 6. Please note the different energy scales in case of the square well and the oscillator. The eigenenergies of the square well scale with $A^{-2/3}$ which is taken into account by the energy unit. No such simple scaling property exists for the oscillator. It is seen from the Figs. 5 and 6 that the shell energy may produce energy gains up to -20 MeV for one sort of particles. Of course, double magic shell closures can only occur, if the two magic numbers correspond to the same f -values.

In Fig. 7 we show lines of constant shell correction energy δE_{shell} in the (N, Z) -plane. Each point corresponds to a minimum of the total energy as a function of f . One should notice that for this case of relatively light bubbles, the shell effects are especially large for almost symmetrical nuclear composition.

In Fig. 8 we display lines of equal energy gain by formation of a bubble. As a reference we use the energy of a spherical LD of the same numbers of neutrons and protons. It is seen that the gain in binding energy may amount to several 100 MeV.

We have still to deal with the crucial question of stability of the bubble solutions with respect to shape deformations. Calculating Strutinsky's shell correction energy (2) for a deformed bubble nucleus implies that we find the eigenvalues of a Schrödinger equation in 3 dimensions or at least (for axial symmetry) in 2 dimensions. Without solving this technical problem we may obtain a valuable insight by describing the deformation dependence of the shell correction energy as suggested by Myers and Swiatecki [11]. In Fig. 9 we display the dramatic effect of the shell correction on the binding energy of a bubble nucleus as a function of the quadrupole deformation. The total LD binding energy of the spherical bubble nucleus is put equal to zero. The LD-part of the energy decreases monotonically as $|\beta_2|$ increases. Adding the shell energy δE_{shell} with Swiatecki's β_2 -dependence produces a valley of about -30 MeV depth. The barriers on both sides of the minimum are about at an energy of -3.9 MeV which leaves us with a barrier height of about 25 MeV. This order of magnitude of the fission barrier implies an almost vanishing probability for spontaneous fission.

What about the other decay modes? β -decay will imply that the system moves along isobaric lines in the (N, Z) -plot towards lower energy. Fig. 8 is particularly instructive in this respect: If a given isobaric straight line cuts a line of constant binding energy twice and if, at the same time, the binding energy between the two points of intersection is lower, a β -stable nuclear bubble lies in between. In Fig. 8 this happens to be the case for $A \geq 600$. If, on the other hand, the energy keeps on lowering along a given isobaric

direction, the β -decays may finally lead to a nuclear composition where bubbles cease to exist. Thus there are cases where bubble nuclei may disintegrate by a series of β -decays and others where the β -decays make them approach a stable composition.

The α -decay, which limits the lifetime of the presently known superheavy nuclei, certainly may also limit the lifetime of bubble nuclei. The penetrability of the Coulomb barrier for an α -particle depends exponentially on the Coulomb potential at $r = R_1$, which has the value $2Ze_0/R_1$. The higher the Coulomb potential, the lower the α -decay probability. For $A = 700$, $Z = 270$, and $R_1 = 11$ fm one finds $2Ze_0^2/R_1 \approx 70$ MeV. We estimate the Q -value to be

$$Q_\alpha := E_{\text{tot}}(Z, N) - [E_{\text{tot}}(Z - 2, N - 2) - 28 \text{ MeV}] \approx 20 \text{ MeV} .$$

Thus the α -particle has to tunnel through a Coulomb barrier whose top is ~ 50 MeV above the tunneling energy. Empirically, the α -decay of heavy actinide nuclei is found to be vanishingly small whenever the emitted α -particle has an energy $Q_\alpha \leq 4$ MeV, i.e. if the energy difference

$$\left(\frac{2Z_{\text{act.}}e_0^2}{R_0(\text{act.})} - Q_\alpha \right) \geq \left(\frac{2Z_{\text{act.}}e_0^2}{R_0(\text{act.})} - 4 \right) \approx 30 \text{ MeV} .$$

This estimate implies that the α -decay probability of typical bubble nuclei is very small due to the especially large Coulomb barrier. Of course, much more careful investigations of the decay modes have to be performed. We may, however, safely say that certain bubble nuclei are expected to have a practically infinite lifetime.

It is intriguing to imagine that stable or at least very long-lived bubble nuclei may exist. Their properties would be a fascinating subject of research. Unfortunately, the masses and charges of the best candidates for bubble structure are so high that there is no hope to produce them. More careful work with the full Hartree-Bogoliubov theory is of course necessary, especially for determining the lower limits of mass and charge numbers of these objects. Even if bubble nuclei can never be made in an earthly laboratory, they might play a role in neutron stars [5].

Finally, there may be bubble structures for mesoscopic systems consisting of some 1000 atoms. This was already conjectured in Ref. [6]. We believe that it may be also of interest to investigate whether shell effects favour the bubble topology for certain mesoscopic systems.

Acknowledgments

K. Pomorski is grateful to the DFG for granting a guest professor position which greatly facilitated the present research. Prior to the 1st April 1997, this research was also modestly supported by the BMBF which is gratefully acknowledged. This work was also partially financed by the Polish Committee of Scientific Research under contract No. 2P03B 049 09. K.D. is grateful for numerous stimulating e-mail messages by M. Weiss.

References

- [1] P.J. Siemens and H.A. Bethe, Phys. Rev. Lett. **18**, 704 (1967).
- [2] J. A. Wheeler, Notebook, unpublished .
- [3] C.Y. Wong, Ann. Phys. (N.Y.) **77**, 279 (1973) (with reference to earlier work).
- [4] P. Bonche, P. H. Heenen, M. Weiss, private communication.
- [5] P. Bonche and D. Vauthérin, Nucl. Phys. **A372**, 496 (1981).
- [6] L.G. Moretto, K. Tso and G.J. Wozniak, Phys. Rev. Lett. **78**, 824 (1997).
- [7] M. Brack, J. Damgaard, A.S. Jensen, H.C. Pauli, V.M. Strutinsky and C.Y. Wong, Rev. Mod. Phys. **44**, 320 (1972).
- [8] P.Ring and P. Schuck, “The Nuclear Many Body Problem”, New York 1980, Springer Verlag.
- [9] P.G. Reinhard and H. Flocard, Nucl. Phys. **A584**, 467 (1995) and ref. therein.
- [10] W.D. Myers and W.J. Swiatecki, Ark. Fys. **36**, 343 (1966).
- [11] W.D. Myers and W.J. Swiatecki, Nucl. Phys. **81**, 1 (1966).

Figures captions.

1. The condition (12) defines a function $v_2(X_0)$ which is shown in the l.h.s. of the figure. The r.h.s. shows the difference $\mathcal{E} = \Delta E_{LD}/E_S(R_0)$ of the LD energy of a bubble of reduced inner radius v_2 and the LD energy of a compact spherical nucleus of radius R_0 .
2. Lines of constant LD-binding energy per particle as a function of (N, Z) . Each point on the lines corresponds to a bubble solution within the LDM. The straight lines in the plot represent isobars.
3. Level scheme as a function of the hole fraction $f = (R_2/R_1)^3$ for the infinite square well plus the spin orbit term (Eqn. 17-19). For 3 values of f (0.12, 0.24, 0.28) numbers are written just above certain s.p. energies e_ν whenever the distance $(e_{\nu+1} - e_\nu)$ exceeds 1.5 energy units. Following the conventional spectroscopic notation the l-values of the levels are given by the letters of the alphabet. The energy unit used takes into account that the eigenvalues of the infinite square well scale with $A^{-2/3}$.
4. As Fig. 5, but for the harmonic oscillator potential. The oscillator frequency ω was determined as a function of f for $A=500$ using relation (16).
5. Shell correction energy as a function of Z (or N) for $f=0.28$ for the infinite square well.
6. As in Fig. 7, but for the harmonic oscillator potential. The frequency of the oscillator was determined by the relation (16) for the mass number $A=500$.
7. Lines of constant shell energy δE_{shell} in the (N, Z) plane. δE_{shell} was calculated for the infinite square well. Each point on the equi-energy lines is evaluated for the hole fraction parameter f corresponding to the minimum of the total energy.
8. Lines of constant energy gain $(\Delta E_{LD} + \delta E_{shell})$ with respect to the energy of a compact spherical LD. The shell correction energy was calculated with the infinite square well potential.
9. LD-energy (dashed line), shell correction energy (dotted line) and total energy (solid line) as a function of the quadrupole deformation β_2 of the outer bubble surface S_1 . The liquid drop energy was minimized with respect of the deformations β_4 and β_6 of the outer surface and β_2 to β_6 of the inner surface. The deformation dependence of the shell correction was taken from Ref. [11].

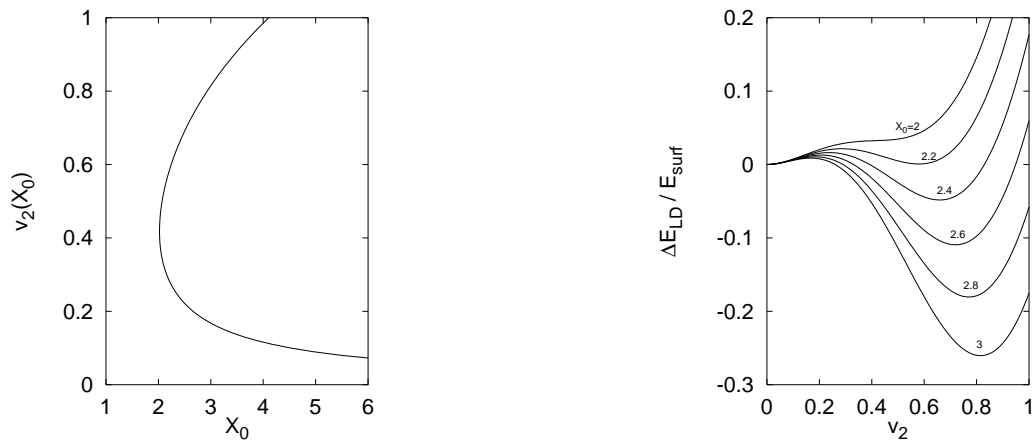


Figure 1:

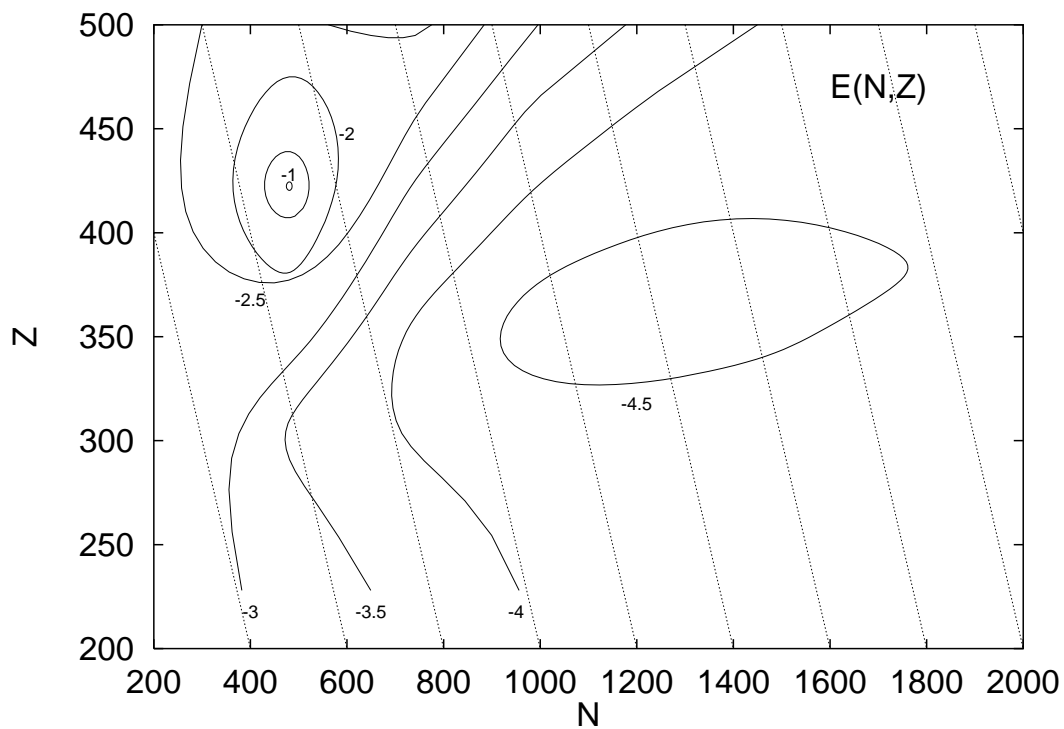


Figure 2:

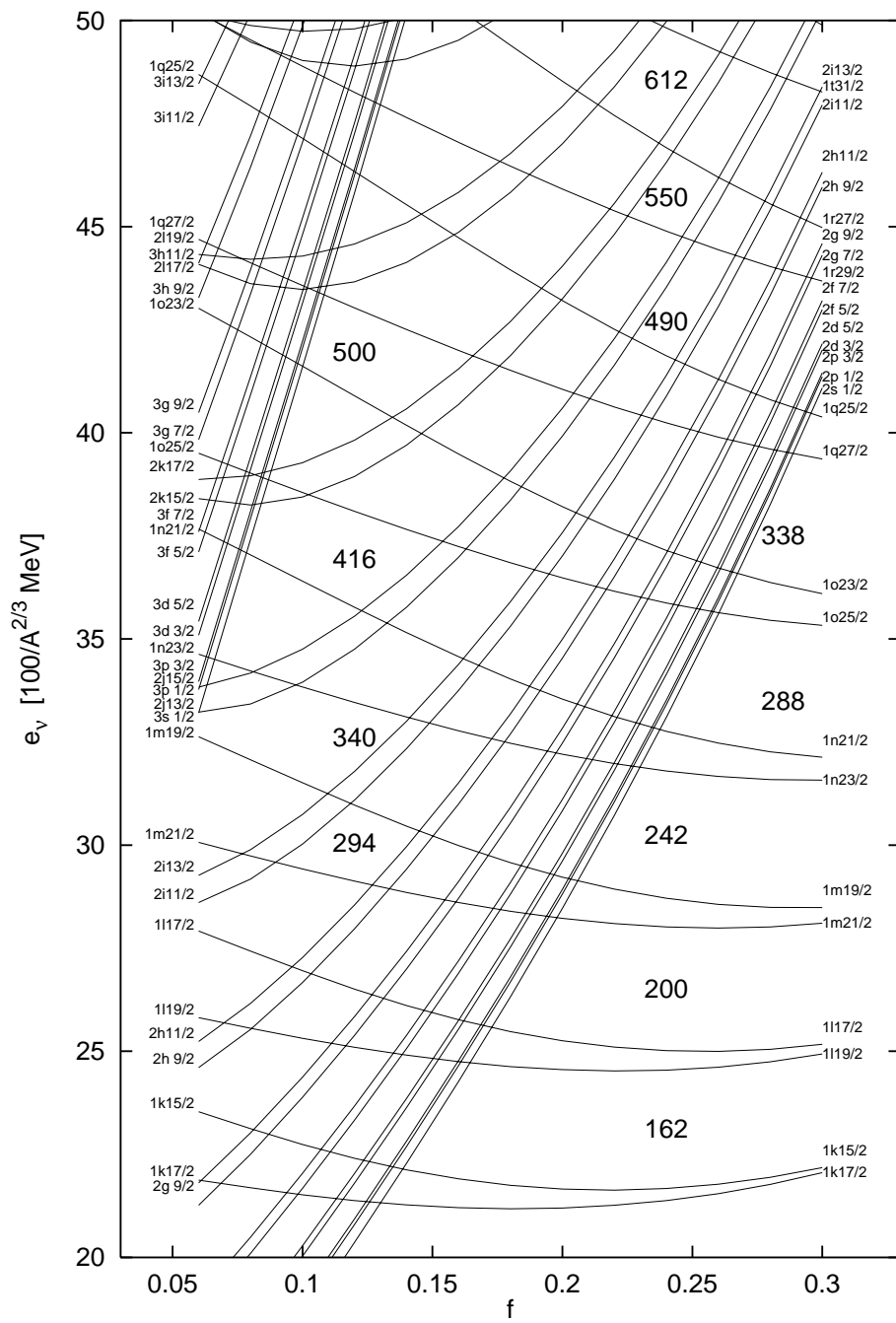


Figure 3:

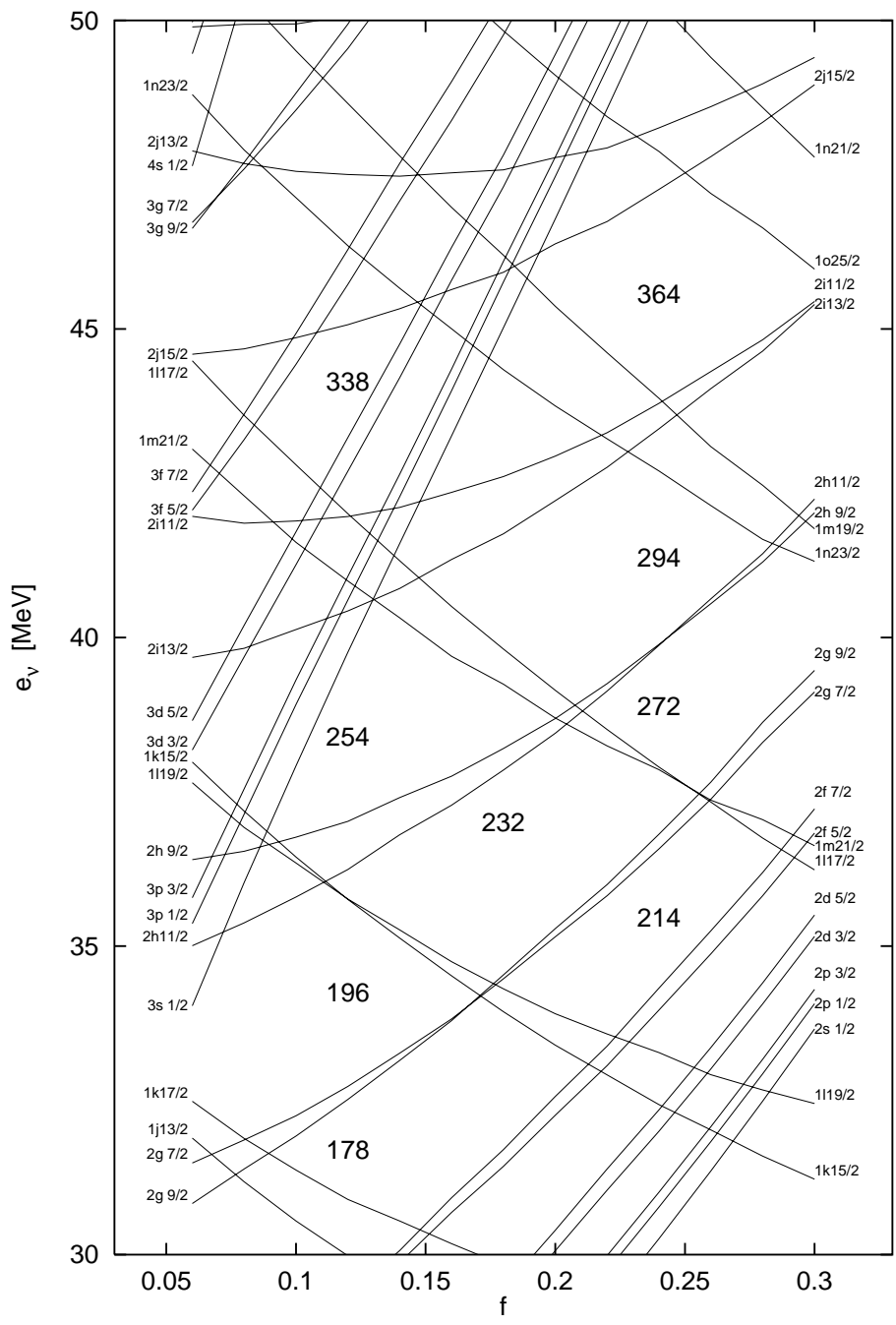


Figure 4:

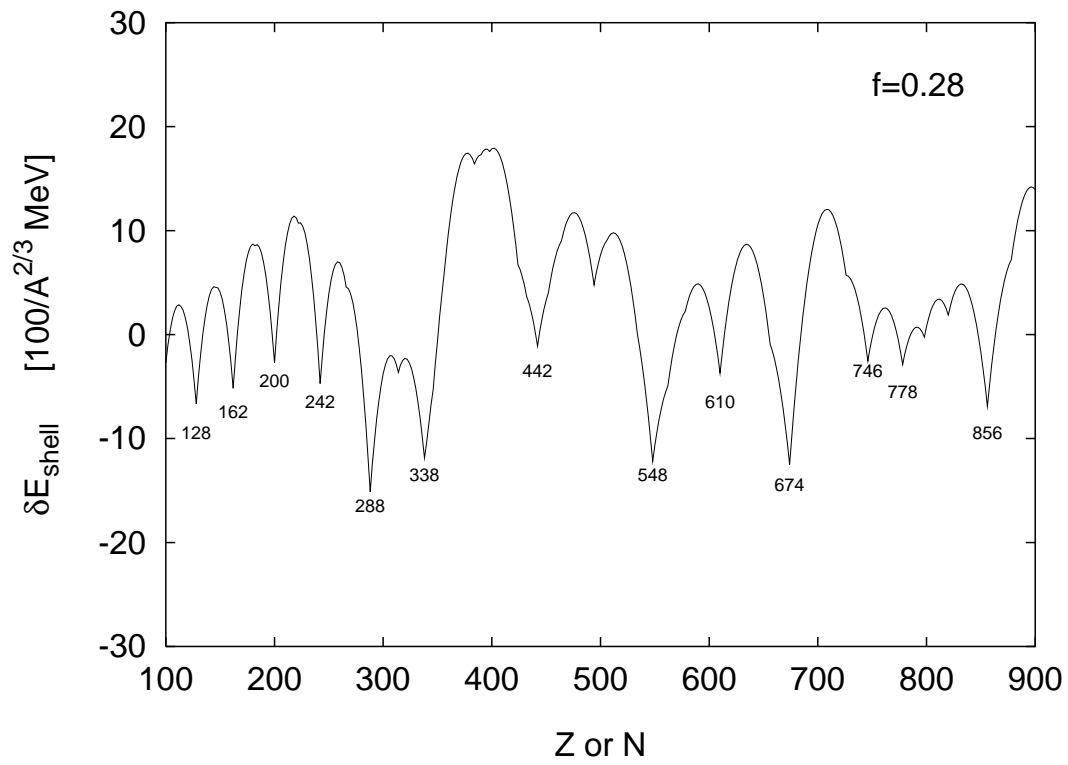


Figure 5:

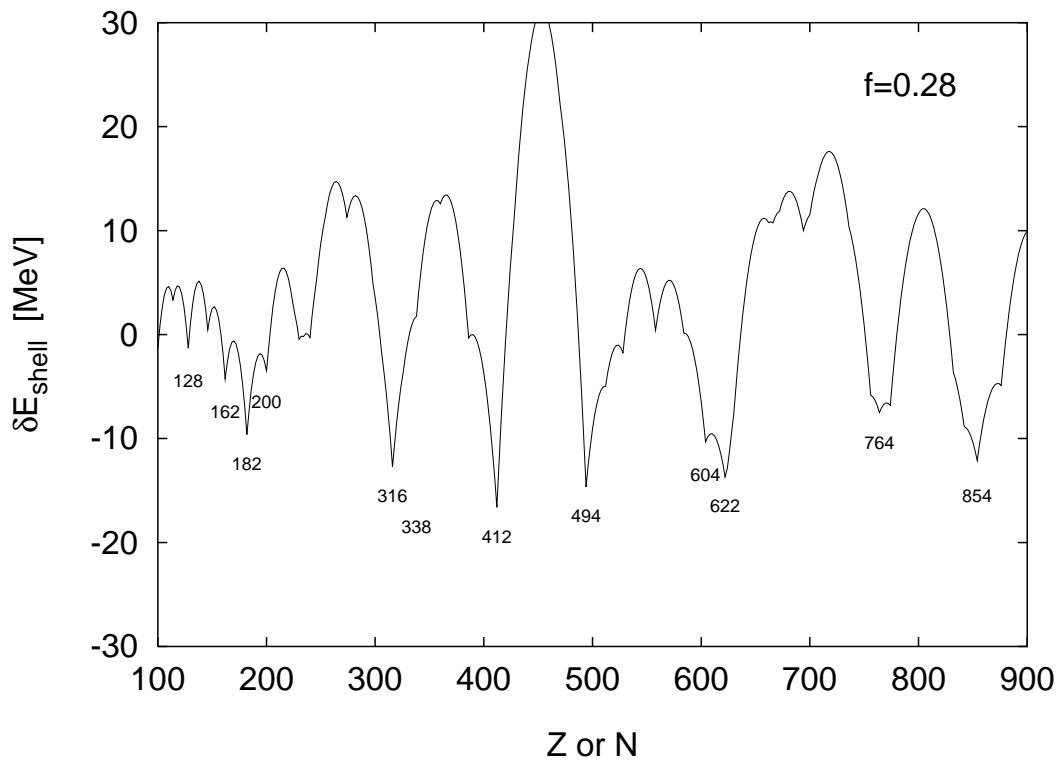


Figure 6:

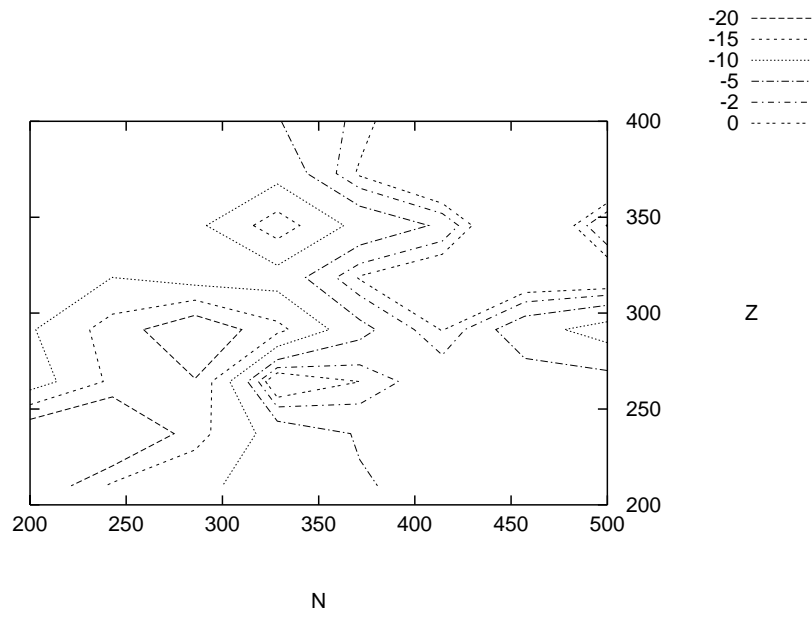


Figure 7:

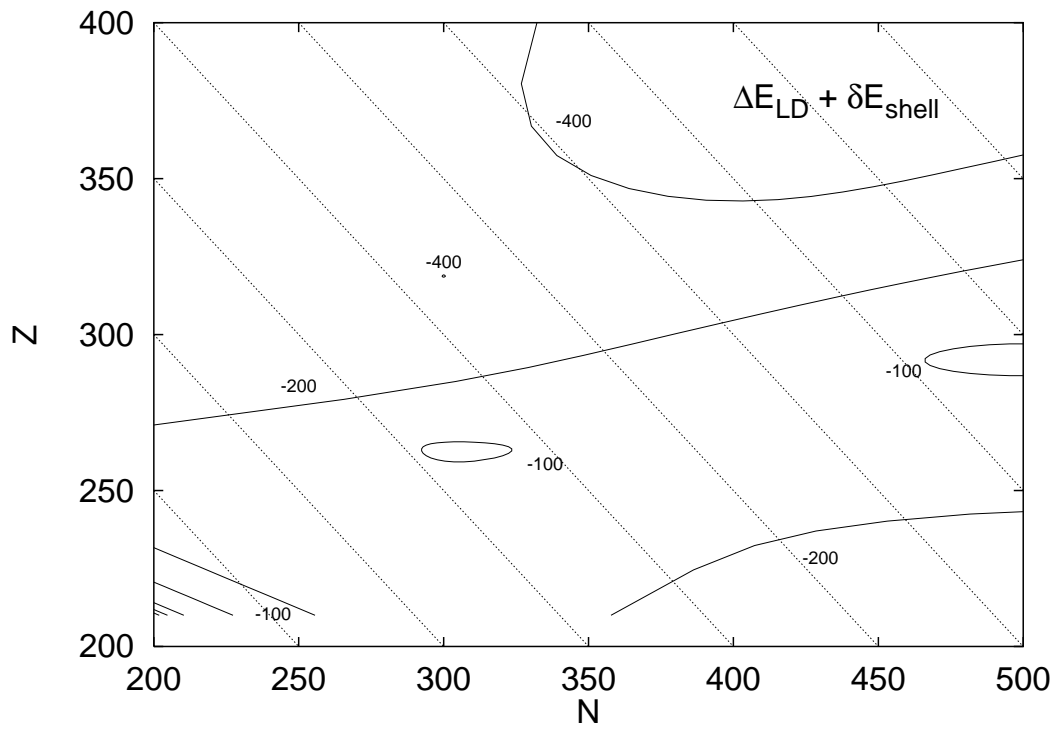


Figure 8:

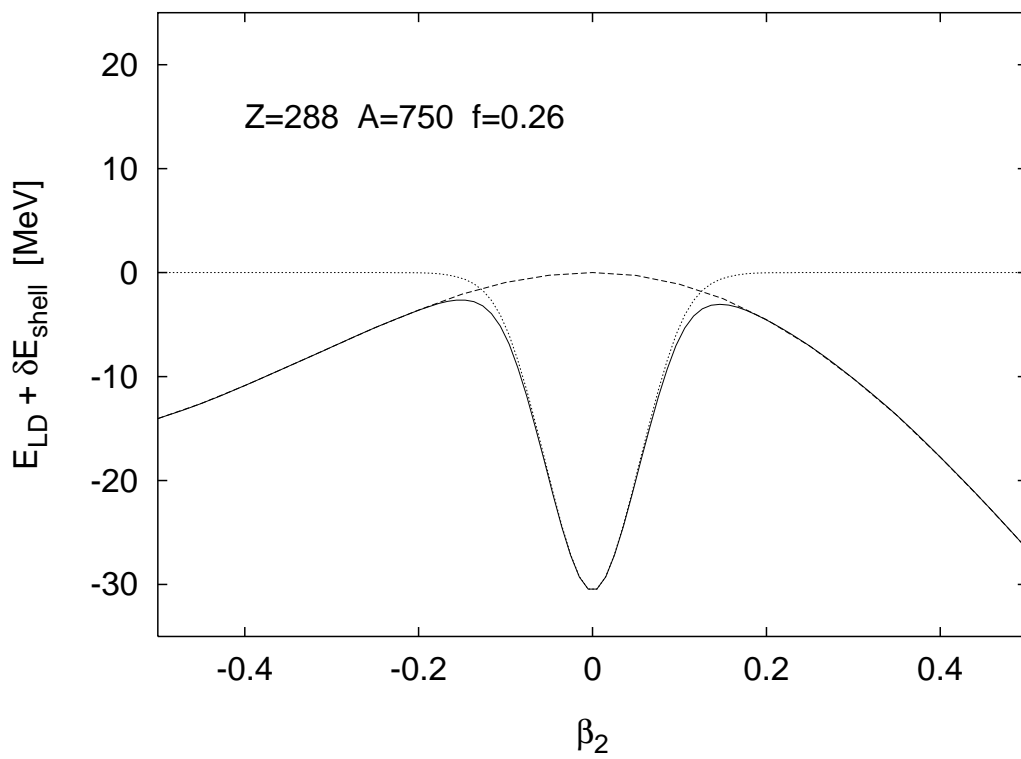


Figure 9: